doi:10.2533/chimia.2011.256 Chimia 65 (2011) 256–259

Investigation of *h*-BN/Rh(111) Nanomesh Interacting with Water and Atomic Hydrogen

Yun Ding[§], Marcella Iannuzzi*, and Jürg Hutter

[§]SCS DSM Prize for best poster

Abstract: Recent STM experiments show that by exposing *h*-BN/Rh(111) nanomesh to water or atomic hydrogen interesting phenomena can be observed. We investigated by Density Functional Theory (DFT) the structure of bare nanomesh as well as in the presence of water clusters and atomic hydrogen. Our simulations allow the correct interpretation of the observed modifications of the STM topography under different tested conditions. For example, we could determine that the frequently observed three protrusions within the pore appearing in STM images obtained after dosing small amounts of water, are most likely determined by water hexamers. We also could confirm that the flattening of the *h*-BN overlayer after dosing atomic hydrogen is determined by the intercalation of the latter between BN and metal, which prevents the effective binding between N and Rh.

Keywords: Atomic hydrogen · Boron nitride nanomesh · Intercalation · STM · Water hexamer

Introduction

The hexagonal boron nitride nanomesh is a corrugated structure with a periodicity of 3.22 nm.[1,2] It is formed by decomposition of borazine onto a clean Rh(111) surface at high temperature. The single layer *h*-BN is regularly corrugated, with 2 nm diameter 'pores' induced by the binding interaction occurring when N atoms are located atop surface Rh atoms. Other regions, which are less tightly bound to the substrate, form the so-called 'wire'. The unit cell is given by 13×13 BN pairs over a 12×12 Rh(111) slab.[2,3] This structure turns out to be very stable not only in gas phase,[2] but also in some liquid solutions.[4] Moreover, the pores are ordered and distantly distributed on the nanomesh, thus making this interface system an interesting candidate for self-assembly of molecule arrays. In experiments, C_{60}[1] and naphthalocyanine[2] have already been successfully deposited into the pore of the nanomesh. In recent STM experiments, after dosing 0.001 L water to bare nanomesh at 34 K, protrusions could be observed in some of the pores. Three protrusions forming an inequilateral triangle, with an average side-length around 4.6 Å, are the most frequently observed geometries. It was immediately noticed that 4.6 Å is close to the distance of second neighbor molecules in ice clusters. Another interesting phenomenon has been observed by dosing atomic hydrogen. In this case, the corrugation disappears, but can be easily recovered after mild annealing, *i.e.* desorbing H.[5]

We studied the interaction of different water clusters in the pore, on the wire, and on the rim of the nanomesh by DFT[6] structure optimization. By simulating the STM topography of the optimized structures, we could identify the most likely aggregates that are observed by STM experiments. We also investigated the interaction of atomic H and the nanomesh, either adsorbing it from above or intercalating it between BN and Rh. By simulated STM topography and by mapping the local work function, we could correlate the experimentally observed flattening of the corrugation with different amounts of intercalated atomic hydrogen.

Method

DFT calculations are performed with the hybrid Gaussian and plane wave (GPW)[7] scheme implemented in CP2K package.[8] We used the revised PBE for the exchange and correlation functional[9] plus van der Waals dispersion corrections computed through the Grimme pair-potential.[10] Goedecker-Teter-Hutter(GTH) pseudopotentials[11] describe the interaction with the cores, where 17 valence electrons are considered for Rh atom, 5 for N, and 3 for B. Double zeta short range molopt basis sets[12] are used for Rh, B and N atoms, and triple zeta for O and H. An energy cutoff of 500 Ry is used to describe the plane wave expansion of the density. Our standard model for the full unit cell of the nanomesh is constituted of one single layer of 13×13 BN pairs and a four layer 12×12 Rh slab, 13on12 model (914 atoms and 19370 basis functions). The characterization of the optimized interface systems by the simulation of STM images within the Tersoff-Hamann approximation[13] allows direct comparison of our results with experiment.[14]

Adsorption of Water Clusters

The optimization of the 13on12 model of the nanomesh reproduce the corrugation of about 1.0 Å. 30% of the overlayer forms the pore region, and lies between 2.1 and 2.3 Å above the Rh(111) surface. Here the BN registry is approximately (top, fcc), and effective binding is possible through the hybridization of the p lone pair of N with the Rh d band. 60% of the BN pairs, instead, belong to the wire, and are more than 3 Å above Rh. In this area the registry

*Correspondence: Dr. M. Iannuzzi
University of Zurich
Institute of Physical Chemistry
Winterthurerstrasse 190
CH-8057 Zurich
Tel: +41 44 635 4479
Fax: +41 44 635 6838
E-mail: marcella@pci.uzh.ch

is mostly (fcc,hcp) or (hcp,fcc) and no significant changes in the electronic structure of free BN are observed. The interaction is dominated by dispersion contributions. The work function computed on the isocurrent surface at about 3 Å over BN is also modulated, being 0.5 eV lower over the pore than over the wire. The modulation of the work function is an important feature of the nanomesh, because the gradient at the rim of the pore is considered to be responsible for the observed trapping of molecules.[14]

To understand the origin of the three protrusions appearing on the experimental STM topography images after dosing water, we optimized and characterized different water clusters in the pore, on the rim, and on the wire. Detailed characterization of all the simulated systems is reported in ref. [14]. Since in the pore the N lone pairs are polarized towards Rh, the adsorption of the water monomer is quite different from what are observed on the wire or on free-standing BN. In the pore, the oxygen is preferentially B-top, and the two OH are one pointing outwards and one parallel to the BN surface. On the wire, instead, one OH points to N in order to form a weak OH···N hydrogen bond (h-bond), 3.38 Å long. On the other hand, when more molecules are present, they aggregate into clusters, since the dominant interactions are the h-bonds among the molecules themselves (–0.2~–0.3eV/h-bond). The adsorption energy to the substrate ranges from –0.1 to –0.2 eV per water molecule, for all the tested systems. In the optimized structure of the water dimer in the pore, both OH of the acceptor O point to nearby N atoms and form OH···N h-bonds. The free OH of the other molecule, instead, points outwards. From the simulated STM topographies reported in Fig. 1, we observe that no protrusion appears for the monomer in the pore, whereas only one protrusion is present in the case of the dimer. Actually, the protrusion appears when the tip sees the sticking out charge of the O lone pair, which occurs when at least one OH is pointing towards the substrate, as in the case of the acceptor molecule of the dimer. Otherwise, when the lone pair is hidden, remaining between the nuclei and the substrate, no bright spot is seen in the STM simulation. We also started an optimization with three water molecules in the pore initially separated such that the initial O–O distance is 4.6 Å, like the distance between the three protrusions in the experimental STM image. However, during the geometry optimization, the water molecules get closer, and finally form a trimer, where three h-bonds connect the O atoms, with O–O distances of 2.8 Å. In the final geometry, only one water molecule has one OH pointing to the substrate, while the other two are pointing upward. Therefore, only one protrusion is seen in the calculated STM image. That rules out the possibility that the three protrusions in the experimental STM image are associated to water trimers. These results indicate that there are features of the STM images related to the orientation of the molecules and the geometry of the adsorbed aggregate can be rationalized. In the cyclic water hexamer, each molecule donates one h-bond to the next molecule in the ring and has one free OH. The distance separating second neighbor O atoms is about 4.7 Å and when adsorbed on BN, every second free OH points to the substrate, forming a weak h-bond with N atoms, about 2.5 Å long. Hence, this geometry is the optimal candidate to reproduce the three protrusions in the STM image. Indeed, the STM simulation obtained from the hexamer optimized above the pore of the nanomesh (adsorption energy –0.117 eV/H_2O) shows the characteristic three bright spots at the right distance (see in Fig. 1c). The water hexamer could also be optimized at the rim and on the wire, with somewhat weaker binding (–0.106 and –0.095 eV/H_2O, respectively). At the rim, the ring of water molecules is quite distorted due to the nanomesh corrugation. This distortion is also evident in the STM analysis of this structure, where the triangle formed by the three protrusions is not equilateral, but shows a certain degree of chirality, which has been observed also in experiment.

Intercalated Atomic H

Hydrogen intercalation below *h*-BN on Rh(111) has been investigated in several steps starting with a single H atom on free standing *h*-BN, where no binding was found for distances longer than 2 Å. Hence, atomic H has to overcome an energy barrier to approach the BN layer that is estimated to be about 0.1 eV. The interaction between atomic H and *h*-BN/Rh was first characterized using a simplified 6on6 model of the pore of the nanomesh. The 6on6 model consists of a slab of seven 6×6 Rh layers, terminated on both sides by a stretched 6×6 BN in (top,fcc) registry. Af-

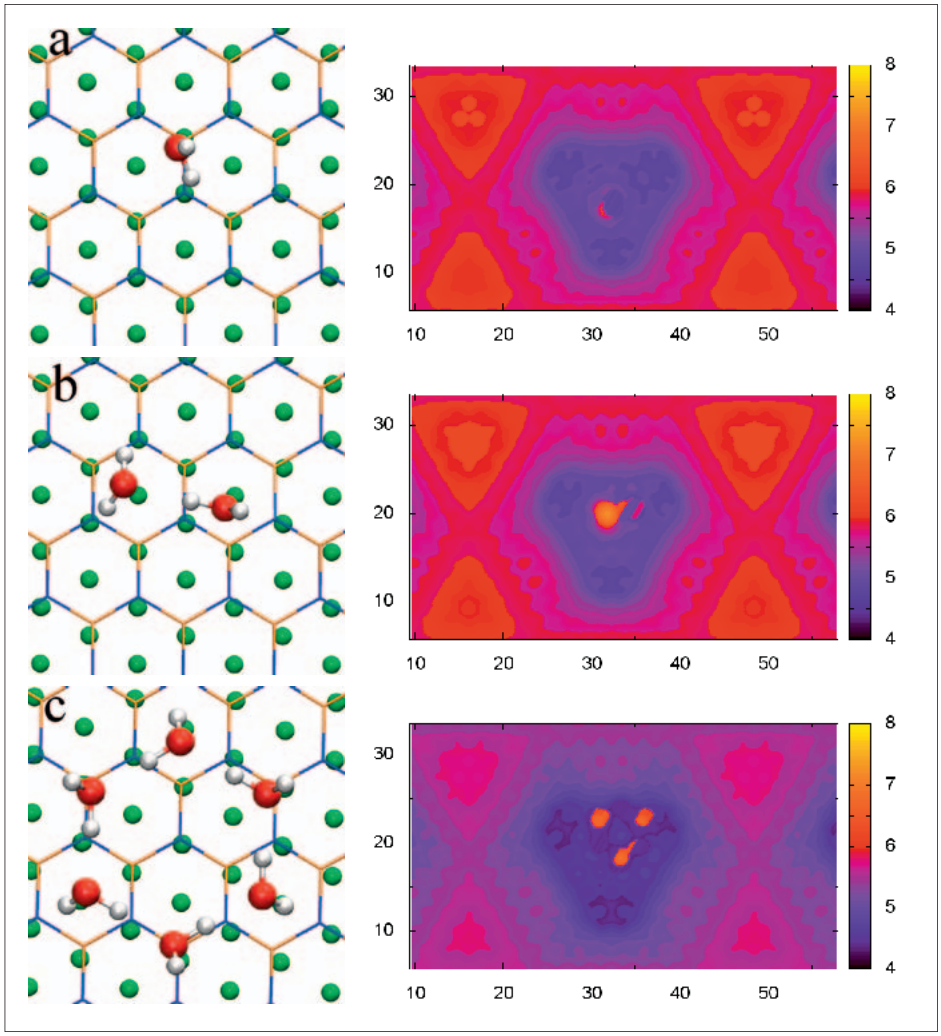

Fig. 1. Configurations (left column) and the corresponding STM topography images (right column) for water monomer (a), water dimer (b) and water hexamer (c) in the pore of the nanomesh. All units are in Å for the STM images.

ter optimization, the BN layer is still flat, the atop N atoms are at 2.2 Å above Rh, and the B atoms are slightly closer to the substrate, with buckling of 0.14 Å. Binding between N and Rh occurs through the hybridization of the N-p orbital's with the metallic d band. The resulting interaction energy between stretched BN and metallic slab amounts to –0.62 eV per BN pair. By locating an H atom in the vacuum space above BN, the interaction turns out to be repulsive for distances larger than 2 Å. Effective binding is obtained only at shorter distances, when H is placed exactly on atop sites, either on N or on B. On N, the binding energy is –1.34 eV, the H–N distance is 1.04 Å, and N is displaced 0.32 Å upwards with respect to the plane of BN. On B, the binding energy is –3.22 eV, H–B is 1.21 Å, and B is displaced 0.64 Å upwards. Also the H monolayer (ML) of 36 atoms (one each BN pair) placed either N-top or B-top can be stabilized. In particular, with N-top coverage, the binding energy per H is –2.13 eV, if computed with respect to the energy of free atomic H. It is, instead, +0.539 eV (positive) if compared to the energy of molecular hydrogen, *i.e.* the adsorption is not convenient in this case. Moreover, the interaction between N and H weakens the binding of nitrogen to the metal, so that the overlayer moves to a B-top position and the BN buckling gets strongly enhanced, with B atoms about 2 Å above the metallic surface, and N atoms at 2.6 Å. By placing the H atoms on top of B atoms, instead, the binding energy is –1.61 eV with respect to atomic H and +0.68 eV with respect to H_2. The overlayer remains in N-top registry, but the buckling is reversed, with B atoms 0.47 Å higher than N atoms.

On pristine Rh(111) surface, H bonding is more effective up to at least one monolayer. The computed binding energy per H atom by increasing the coverage is –2.87 eV for ¼ ML, –2.82 eV for ½ ML, and –2.74 eV for 1 ML. Different adsorption sites have been tested, finding that fcc hollow sites are slightly favored (–2.74 eV for 1 ML fcc vs. –2.72 eV for 1 ML hcp), in accordance with ref. [15]. These results, together with the experimental findings, suggest that, after exposure to atomic H, a certain amount of H could be intercalated between BN and Rh(111). Hence, one monolayer of intercalated H has been added to the 6on6 model with BN in (top,fcc) registry. The presence of H in the interlayer breaks the chemical bonding between the metal and N. Therefore, the BN layer loses contact with the substrate and is displaced higher up. The intercalated H atoms may occupy either fcc or hcp sites. In particular, with one ML of fcc H, the binding energy per H atom is –2.32 eV and the BN is about 3.4 Å above Rh, whereas by intercalating one hcp ML, the binding energy per H is –3.3 eV and BN stays at 3.3 Å from Rh.

Table 1. Binding energy (E_b), average distance of N atoms from Rh surface (Rh-N), peak-to-peak corrugation of the overlayer (dh), and modulation of the work function about 7.5 Å above the Rh slab (dWF) computed for the optimized nanomesh unit cell (13on12) in the presence of different amounts of intercalated H. The clean system (without H) is characterized by Rh-N=2.9 Å, dh=1.1 Å, and dWF=0.4 eV.

	E_b [eV/H]	Rh-N [Å]	dh [Å]	dWF [eV]
¼ ML fcc	-2.57	3.1	1.0	0.3
½ ML fcc	-2.59	3.2	0.3	0.18
1 ML fcc	-2.62	3.4	0.2	0.13
1 ML hcp	-2.60	3.4	0.14	0.13

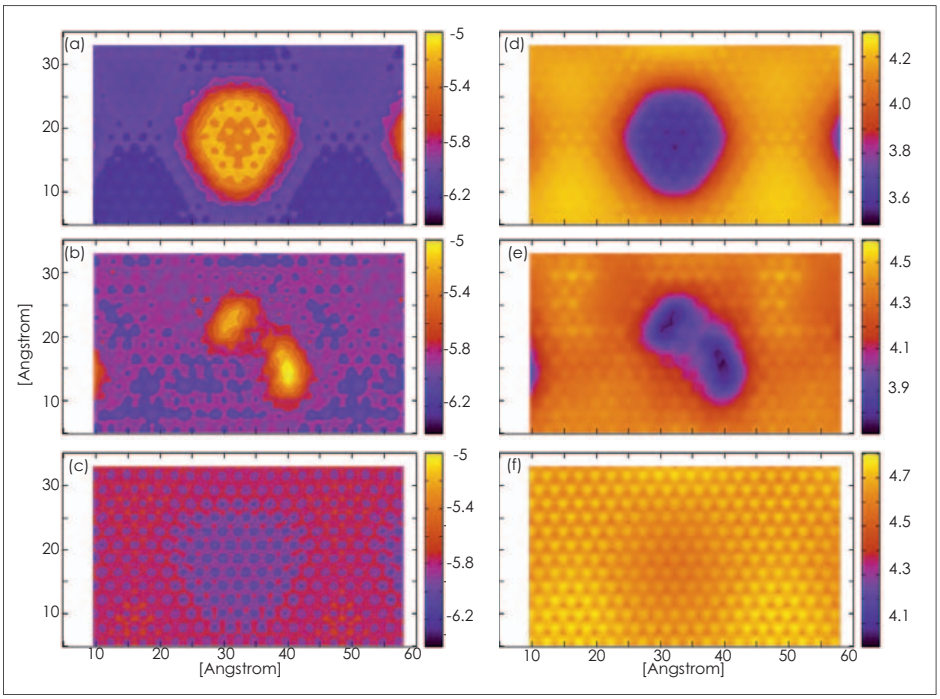

Fig. 2. STM (left) and work function (right) images for bare nanomesh (a, d), nanomesh+¼ ML H in the interlayer (b, e) and with 1ML intercalated H (c, f). The color map values are in Å for STM and eV for work function.

Finally, the nanomesh structural changes due to intercalation have been investigated by distributing H on either fcc or hcp hollow sites, with different densities (¼ ML, ½ ML, and 1 ML) between the *h*-BN layer (13×13 units) and the four layer 12×12 Rh(111) slab. All the structure optimizations led to H–Rh bonding configurations, where the mean *h*-BN layer – Rh distance progressively increases and the corrugation, as well as the modulation of the work function between pore and wire, are significantly reduced by increasing the amount of intercalated H (see Table 1).

The fact that slight modulation of the work function persists is an indication of different polarization effects of N electronic charge on Rh-top sites with respect to N on fcc or hcp sites, in spite of the presence of H and the larger layer distance. The simulated STM topographies of the clean nanomesh, the system with ¼ ML, and the one with 1 ML of intercalated H are reported in Fig. 2. In the same figure the work function maps calculated on the same iso-current surfaces are displaced. The fundamental feature of the H intercalated system is the drastic reduction of the *h*-BN corrugation amplitude by a factor of five from 1.1 Å to 0.2 Å, which supports the picture of H intercalation drawn from the experiment. This structural change directly influences the electrostatic potential, whose corrugation amplitude within the nanomesh unit cell drops from 380 meV to 130 meV at a distance of 7.5 Å above the *h*-BN layer. Thus the strength of the lateral dipole rings in the *h*-BN layer, which are located at the sites of the highest corrugation gradient and which are the source of the molecular traps of the *h*-BN/Rh(111) nanomesh, is expected to be reduced by about 90%. The experimentally observed disappearance of the σβ band in UPS after H intercalation is also confirmed by theory, where the σ band splitting between the hole and wire derived N-p_x DOS decreases with the amount of intercalated H, finally rendering both DOS experimentally indistinguishable for coverage larger than ½ ML (Fig. 3).

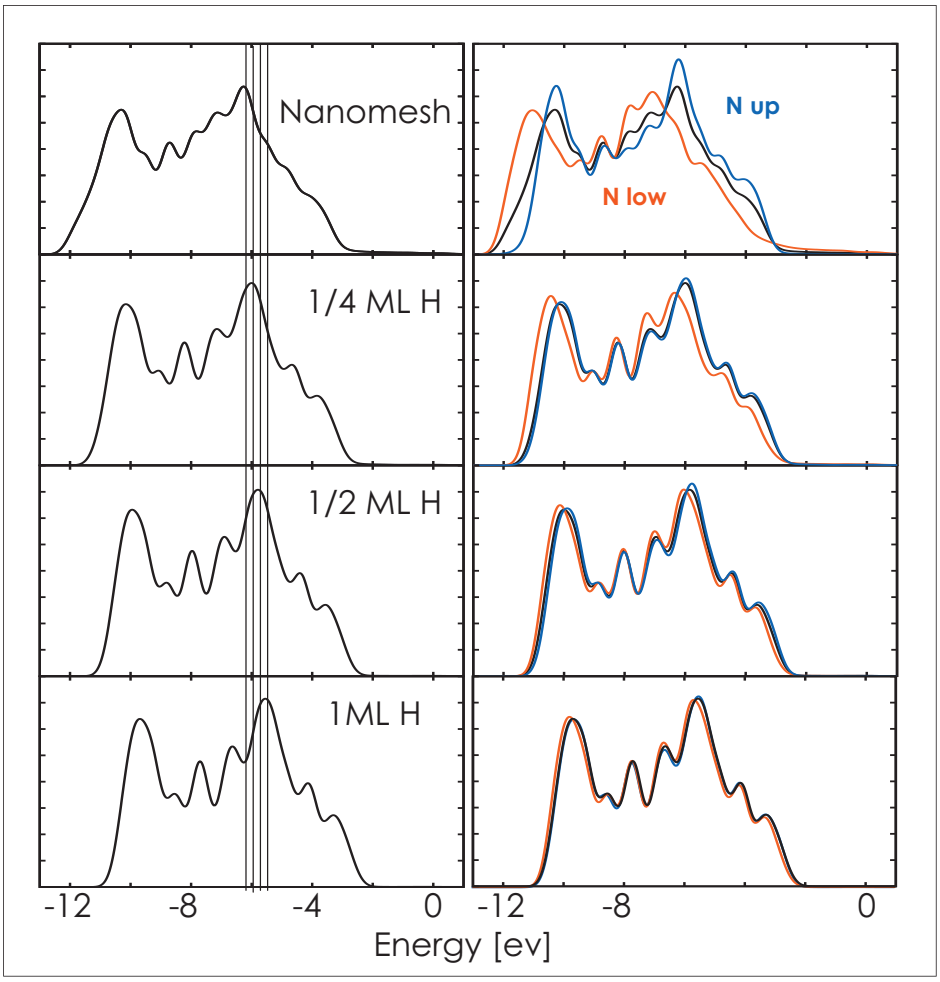

Fig. 3. N-p_x projected density of states (DOS) for the bare nanomesh, the nanomesh with ¼ ML, ½ ML and 1 ML intercalated atomic H, respectively.

Conclusion

We presented a DFT study of the interaction of water clusters and atomic hydrogen with *h*-BN/Rh nanomesh. By studying the adsorption of different water clusters and comparing the calculated STM topography to the experiment, we conclude that the water hexamer is the best fit for the three protrusion geometries frequently observed in experimental STM. More importantly, we are able to associate specific feature of the STM images to the orientation of the water molecules in the cluster, *i.e.* to the position of the H atoms. The investigation of the interaction with atomic H indicates that the most probable reason for the flattening is the intercalation. By distributing different amounts of H in the interlayer, the reduction of the corrugation and the change in the work function modulation observed in experiment have been reproduced, as well as the disappearance of the pore signal in the N-p projected density of states.

Acknowledgement

The authors thank Prof. Dr. Thomas Greber, Dr. Haifeng Ma and Dr. Thomas Brugger for fruitful discussions. This work is supported by Swiss National Science Foundation under Grant No. CRSI20_122703. The authors thank Swiss National Supercomputer Centre (CSCS) and University of Zurich for generous computational resources.

Received: January 24, 2011

[1] M. Corso, W. Auwärter, M. Muntwiler, A. Tamai, T. Greber, J. Osterwalder, *Science* **2004**, *303,* 217.
[2] S. Berner, M. Corso, R. Widmer, O. Groening, R. Laskowski, P. Blaha, K. Schwarz, A. Goriachko, H. Over, S. Gsell, M. Schreck, H. Sachdev, T. Greber, J. Osterwalder, *Angew. Chem., Int. Ed.* **2007**, *46,* 5115.
[3] R. Laskowski, P. Blaha, T. Gallauner, K. Schwarz, *Phys. Rev. Lett.* **2007**, *98,* 106802.
[4] a) O. Bunk, M. Corso, D. Martoccia, R. Herger, P. R. Willmott, B. D. Patterson, J. Osterwalder, J. F. van der Veen, T. Greber, *Surf. Sci.* **2007**, *601*, L7; b) R. Widmer, S. Berner, O. Gröning, T. Brugger, J. Osterwalder, T. Greber, *Electrochem. Commun.* **2007**, *9,* 2484.
[5] T. Brugger, H. F. Ma, M. Iannuzzi, S. Berner, A. Winkler, J. Hutter, J. Osterwalder, T. Greber, *Angew. Chem., Int. Ed.* **2010**, *49,* 6120.
[6] W. Kohn, L. J. Sham, *Phys. Rev.* **1965**, *140,* A1133.
[7] G. Lippert, J. Hutter, M. Parrinello, *Mol. Phys.* **1997**, *92,* 477.
[8] CP2K version 2. 1. 289 (Development Version), the CP2K developers group (2010). CP2K is freely available from *http://cp2k.berlios.de/.*
[9] a) J. P. Perdew, K. Burke, M. Ernzerhof, *Phys. Rev. Lett.* **1996**, *77,* 3865; b) Y. K. Zhang, W. T. Yang, *Phys. Rev. Lett.* **1998**, *80,* 890.
[10] S. Grimme, *J. Comput. Chem.* **2006**, *27,* 1787.
[11] a) S. Goedecker, M. Teter, J. Hutter, *Phys. Rev. B* **1996**, *54,* 1703; b) C. Hartwigsen, S. Goedecker, J. Hutter, *Phys. Rev. B* **1998**, *58,* 3641; c) M. Krack, *Theor. Chem. Acc.* **2005**, *114,* 145.
[12] J. VandeVondele, J. Hutter, *J. Chem. Phys.* **2007**, *127*, 114105.
[13] a) J. Tersoff, D. R. Hamann, *Phys. Rev. Lett.* **1983**, *50,* 1998; b) J. Tersoff, D. R. Hamann, *Phys. Rev. B* **1985**, *31,* 805.
[14] H. F. Ma, Y. Ding, M. Iannuzzi, T. Brugger, S. Berner, J. Hutter, J. Osterwalder, T. Gerber submitted.
[15] M. Fukuoka, M. Okada, M. Matsumoto, S. Ogura, K. Fukutani, T. Kasai, *Phys. Rev. B* **2007**, *75*, 235434.